THE STRUCTURAL DESIGN OF TALL BUILDINGS
Struct. Design Tall Build. **9**, 343–363 (2000)

MODELING OF TWO-CELL CORES FOR THREE-DIMENSIONAL ANALYSIS OF MULTI-STORY BUILDINGS

HARITON XENIDIS, KOSTAS MORFIDIS AND IOANNIS E. AVRAMIDIS*
Department of Civil Engineering, Aristotle University of Thessaloniki, 54006 Thessaloniki, Greece

SUMMARY

The reliability of simplified models for single-cell cores, and particularly for open and semi-open U-cross-section cores, has been the subject of many research papers in the recent past. In contrast, on an international level, only little mention has been made of the efficiency of such models for multi-cell cores of multi-story R/C buildings. This paper evaluates and comments on the reliability of several simplified models for open two-cell cores that are often used in practice. The models examined are: (a) models composed of equivalent columns in alternative configurations; (b) models composed of panel elements; and (c) finite shell element models with one element for each flange in each story. These models are compared with one another and with the solution considered accurate, which is the one obtained by using a finite element method consisting of an adequately dense mesh of finite shell elements. The conclusions obtained refer to both the simplified modal response analysis and the multi-modal response spectrum analysis, while the specific assumptions for the numerical investigations are compatible with the provisions of modern seismic design codes. Copyright © 2000 John Wiley & Sons, Ltd.

1. INTRODUCTION

1.1. Modeling ordinary R/C buildings

The penetration of the finite element method into almost all fields of structural computation has not yet been able completely to replace the use of simplified modeling and analysis methods. Although these methods are less accurate, they generally satisfy the reliability requirements for conventional R/C buildings. Widely accepted models for the analysis of multi-story buildings with planar shear walls and cores are: equivalent frame models, also referred to as wide column analogy, and panel element models. Also—in some cases—core models consisting of a sparse mesh of finite elements are used. Mainly the use of the equivalent frame model has been a major success. This model was devised for the analysis of planar shear walls approximately four decades ago (Beck, 1962; MacLeod, 1967; Schwaighofer 1969). It provides a simple line-member model that represents well the behavior of single or coupled planar shear walls and makes analysis by means of conventional frame programs possible (Schwaighofer and Microys, 1969). The simplicity and effectiveness of this model has almost self-evidently led to the extension of its application to composite shear walls (cores) in three-dimensional analysis of multi-story buildings (Heidebrecht and Swift, 1971; MacLeod, 1973; MacLeod and Green, 1973; MacLeod, 1976; MacLeod and Hosny, 1977; MacLeod, 1977; Stafford-Smith and Abate, 1981; Lew and Narov, 1983; Stafford-Smith and Girgis, 1984). However, soon, serious deficiencies in the performance of this model were detected. Several investigations on this matter have shown that application of this model to open, semi-open and closed building cores

* Correspondence to: Prof. I. E. Avramidis, Department of Civil Engineering, Aristotle University of Thessaloniki, Thessaloniki, 54006 Greece.

Received February 1999
Accepted March 2000

subjected to strong torsion leads to inaccurate or even unacceptable results (Girgis and Stafford-Smith, 1979; Stafford-Smith and Girgis, 1986; Avramidis, 1991; Avramidis and Xenidis, 1991; Xenidis *et al*., 1992; Xenidis and Avramidis, 1992; Xenidis *et al*., 1993). Also, significant deviations from the correct solution are observed for planar shear walls with varying width along their height or with irregularly distributed openings (Xenidis *et al*., 1994). Furthermore, it should be noted that the equivalent frame model for a given core is not unique. Quite the contrary, it depends on certain necessary assumptions that can lead to different spatial frame models (Avramidis, 1991). The differences between the possible models concern: (a) the number of equivalent columns; (b) their location in the core cross-section; and (c) the cross sectional properties of equivalent columns and interconnecting auxiliary beams (links) used at the story levels. The reliability and efficiency of a series of various equivalent frame models for open, mainly U-shaped cores have been investigated in depth in the recent past (Avramidis and Xenidis, 1991; Xenidis *et al*., 1992; Xenidis and Avramidis, 1992; Xenidis *et al*., 1993; Avramidis, *et al*., 1997; Xenidis, *et al.*, 1998; Xenidis and Avramidis, 1999). On the contrary, the reliability of equivalent frame models for multi-cell cores, and especially for open two-cell cores is very poor, although such cores are very often encountered in practice.

1.2. Scope of the paper

When dealing with double- or multi-cell cores, the problem of choosing between the various alternatives in order to establish a satisfactory equivalent frame model becomes even more difficult and complicated than in case the of non-regular yet planar shear walls. In contrast to the simple, one-cell U-section core, for which web and flanges are clearly identified, in multiple-cell cores this distinction is in general vague, if possible at all. This fact leads to many, rationally possible locations of the equivalent columns in plan-view (Avramidis, 1991), and, consequently, to a large number of possible spatial frame models, the reliability of which is *a priori* unknown. In addition, there is a high risk of inefficient choice of the geometric and elastic characteristics of the equivalent columns' and auxiliary beams' cross sections, which can lead to completely false representation of the actual behavior of the core in space.

The scope of this paper is to present a systematic examination of the reliability and efficiency of simplified models for the two-cell core with open cross-section, which is often used in practice for housing elevators or service ducts. Examined are: (a) models consisting of alternative configurations of equivalent columns; (b) models using panel elements; and (c) models composed of a sparse mesh of finite shell elements (one element per flange and story). These models are compared with one another and with the solution considered accurate. Here, the 'accurate' solution is assumed to be that obtained by modeling the core by an adequately dense mesh of finite shell elements. The conclusions drawn refer to both simplified modal response analysis (also referred to as equivalent static analysis) and multi-modal response spectrum analysis (briefly: response spectrum analysis), while all specific assumptions made comply with the provisions of modern seismic design codes.

It should be emphasized here that previous evaluations of the efficiency of equivalent frame core models were mostly based on comparisons of calculated stresses for each individual flange of the core separately. This common method for assessing the reliability of models was dictated by the fact that the dimensioning (i.e. the calculation of the amount of reinforcement and various checks at cross-section level) which followed the analysis were performed using programs designed for rectangular R/C cross sections. Today, many programs are available that allow for dimensioning of arbitrarily shaped R/C sections as a unit. Therefore, it is no longer necessary to compare response stresses separately for each flange of the core section. The efficiency of the modeling variants can be checked by comparison of the resultant cross-sectional forces in the core as a whole. By shifting the comparison from individual flanges to the composite cross-section, the observed deviations of the simplified models

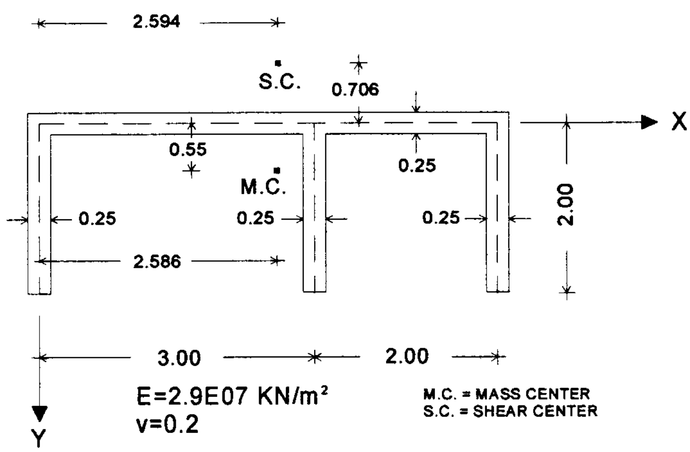

Figure 1. Plane view of the investigated two-cell core

measured up to the exact solution become smaller—as has been already pointed out (Xenidis *et al.*, 1998)—and the frame models become more acceptable in engineering practice.

2. STRUCTURAL SYSTEMS AND MODELS

2.1. Basic modeling assumptions

It should be noted that the largest deviations of the various simplified core models are observed when investigating isolated cores. In practice, however, a core is generally embedded in the frame skeleton of the building and connected to it through beams and slabs. This connection generally reduces the resulting torsional deformations of the core, which are the main source of inaccuracies in the models' responses to external loading. As a consequence, the deviations of the final results become smaller. In order to evaluate the differences in the final effectiveness of simplified models, results are presented that concern both: isolated cores and cores integrated into the building's load bearing system. In the present paper, all analyses are carried out using the two-cell open core shown in Figure 1 and the 10-story building shown in Figure 2.

The investigated isolated core (Figure 1) is 10-story high, and absolutely fixed at its base. The 1st story has a height of 5·0 m, while the height of each of the other stories is 3·0 m. For static analysis, the loading consists of two equal horizontal forces of 300 kN each along the positive and negative *y*-direction, respectively, at the two opposite edges of the core's top. For the response spectrum analysis, the design spectrum of the Greek seismic design code (Manos, 1994) is used with the following data: soil A, seismic zone II (A = 0·16*g*), importance factor $\gamma = 1$, foundation coefficient $\theta = 1$, damping coefficient = 5% and seismic load reduction factor $q = 3$. The seismic excitation was considered to act along the *x*-direction, while the core mass $m = 100\,\mathrm{kN\,s^2\,m^{-1}}$ is considered to be concentrated at the level of each story and placed at a distance of 5 m from its mass center in the positive *y*-direction. The deliberate choice of an eccentric location for the core's mass is aiming to produce a realistically high torsional deformation in order to reveal the deficiencies in performance of the simplified models under consideration. Because, as the study of U-shaped cores has shown (Stafford-Smith and Girgis, 1936; Avramidis, 1991), deficiencies increase with increasing torsion.

The investigated 10-story building (Figure 2) does not have the complexity of real buildings, which might have complicated the derivation of clear and unambiguous conclusions. However, it does have the basic characteristics of typical multi-story R/C buildings. The eccentric location of the open two-

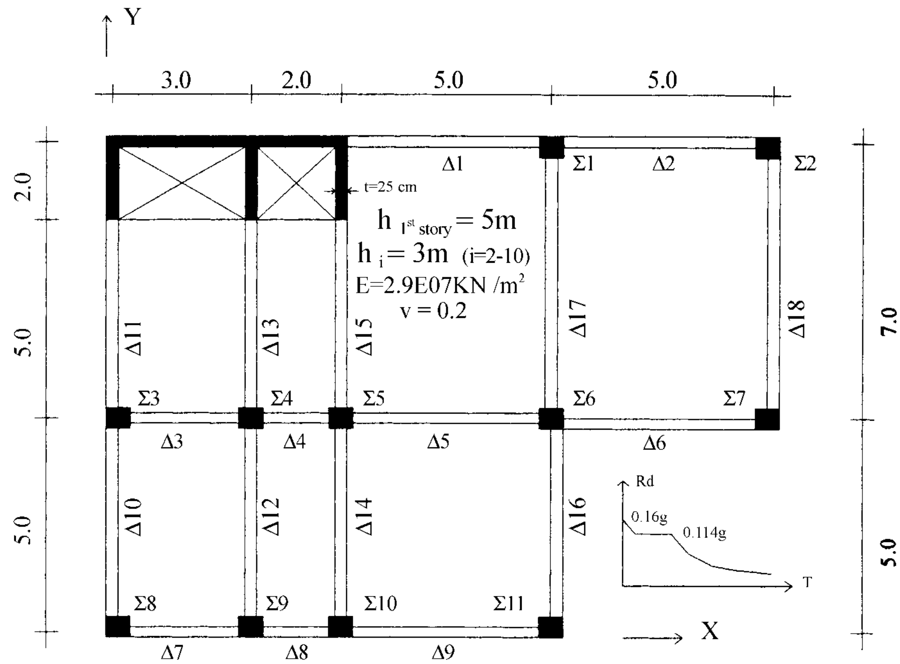

PERMANENT LOAD ON SLABS : 15 KN / m ^{2}

Columns: stories 1^{st}- 4^{th} 60/60, 5^{th}- 7^{th} 50/50, 8^{th}- 10^{th} 40/40

Beams: 1^{st} story 25/80, stories 2^{nd}- 4^{th} 25/70, 5^{th}- 10^{th} 25/60

Figure 2. 10-story building

cell core at the upper left corner of the plan view should, of course, be avoided in real constructions. Here, it serves the purpose of identifying the highest possible deviations of non-isolated core models. As already proven in previous papers (Avramidis, 1991; Avramidis and Xenidis, 1991), deviations become larger if the cores are subjected to intense torsion due to the asymmetric plan-view configuration of the building.

In modeling the building, the following simplifications are made: (a) the floor slabs are assumed to act as absolutely rigid diaphragms (no in-plane deformations); (b) the contribution of the slabs to the flexural stiffness of the beams has been taken into account assuming co-operating widths of 1·25 m for the interior beams and 0·75 m for the beams on the perimeter; (c) flexural as well as axial, shear and torsional deformations in line-elements have been taken into account; (d) small eccentricities in the connections of beams and columns are neglected; and (e) the seismic loads are considered to act on the mass centers ignoring openings in the core area or other eccentricies, accidental or not.

The magnitudes and the vertical distribution of the horizontal seismic loads for the equivalent static analysis of the building are determined according to the design spectrum of the Greek seismic design code (Manos, 1994) by using the uncoupled fundamental period of the building. As can be seen in Table I, these equivalent static loads are not exactly the same for all models. They are slightly different because of slight differences in the fundamental periods of the various models.

All calculations are performed using the linear static and dynamic analysis programs SAP90 (Wilson and Habibullah, 1992a) and ETABS (Wilson and Habibullah, 1992b).

Table I. Fundamental uncoupled natural periods for Models No. 1–No. 6 and corresponding seismic loadings for the equivalent static analysis of the building in the x-direction (a) and y-direction (b)

		No. 1	No. 2	No. 3	No. 4	No. 5	No. 6
	T_x	0·7076	0·7244	0·7092	0·7087	0·7061	0·7056
	Vo	2226·85	2192·22	2223·46	2224·39	2229·87	2231·07
	10	445·07	430·35	446·10	446·30	446·98	447·05
S	9	395·20	383·81	395·60	395·78	396·66	396·82
t	8	343·37	335·05	343·40	343·58	344·37	344·62
o	7	290·23	284·68	290·10	290·25	291·08	291·11
r	6	238·55	235·48	238·10	238·18	238·91	239·11
i	5	187·63	186·73	187·00	187·08	187·72	187·86
e	4	139·34	140·25	138·70	138·74	139·25	139·21
s	3	97·26	99·54	96·20	96·29	96·70	96·80
	2	60·03	63·16	59·00	58·99	59·20	59·26
	1	30·19	33·17	29·20	29·19	28·98	29·21

(a)

		No. 1	No. 2	No. 3	No. 4	No. 5	No. 6
	T_y	0·8400	0·8522	0·6846	0·8394	0·8300	0·8285
	Vo	1986·15	1967·17	2276·43	1987·15	2002·07	2004·52
	10	368·48	357·31	442·20	367·39	374·87	375·40
S	9	336·31	327·78	396·70	335·79	341·84	342·30
t	8	300·33	294·09	348·60	300·25	304·91	305·30
o	7	260·44	256·22	298·20	260·69	264·07	264·40
r	6	219·12	217·01	247·50	219·49	221·38	221·60
i	5	176·26	176·03	196·60	176·75	177·28	177·50
e	4	134·32	135·84	147·50	135·04	134·37	134·50
s	3	96·91	100·02	103·50	97·46	95·59	95·70
	2	62·06	66·24	64·00	62·40	59·53	59·60
	1	31·87	36·62	31·60	31·90	28·24	28·30

(b)

2.2. *Core modeling with finite shell elements (Model No. 1)*

As already mentioned, the basis for comparison and reference solution are served by a core model consisting of an adequately dense mesh of finite shell elements (Model No. 1). Based on preliminary solutions, a mesh with elements of $1{\cdot}0\,\text{m} \times 1{\cdot}0\,\text{m}$ for the web and the flanges of the core was considered adequate (Avramidis *et al*., 1997; Xenidis *et al*., 1998). In addition, in order to enforce the rigid diaphragm behavior at the story levels, auxiliary axially rigid beams were used with practically 'infinite' flexural and shear stiffnesses in the horizontal x–y plane, while these properties in the vertical x–z and y–z planes were set to zero. It should be noted that, in order to be able to compare results, instead of the element stresses themselves, the balanced, statically equivalent nodal forces of the shell elements are used, which are automatically calculated by SAP90. The resultants of the balanced equivalent nodal forces can than be compared with stress resultants from frame models (bending moments M, shear forces Q, and axial forces N).

2.3. *Core modeling with equivalent frames (Models No. 2, No. 3 and No. 4)*

The basic rules for the creation of models using equivalent frames for shear walls and cores are described in detail in the literature (see, for example, MacLeod, 1977 and Avramidis, 1991). Figure 3

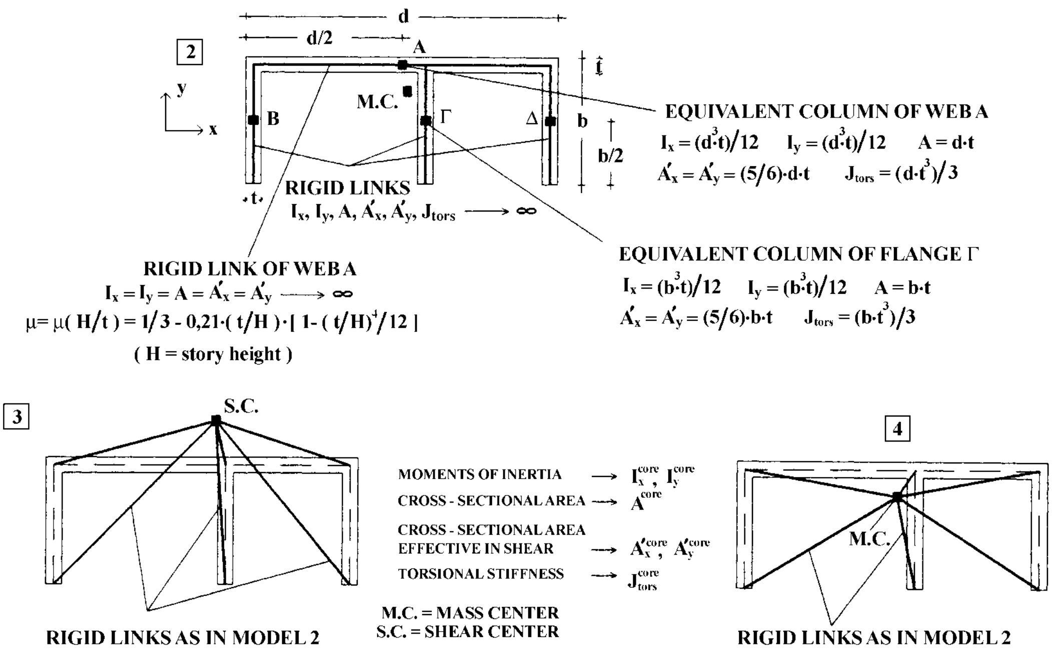

Figure 3. The three investigated equivalent frame models (Models No. 2–No. 4)

represents a plan-view of the three equivalent frames models, No. 2, No. 3 and No. 4, whose performance is investigated in the present paper. Model No. 2, which is the first frame model used for cores, can be characterized as the 'classical model'. The other two models are picked out because of the fact that they are integrated in many professional structural analysis programs, and, for that reason, the evaluation of their reliability is of major importance for the design engineer in everyday practice.

At this point the reader should be reminded of the important role played by the absolutely stiff beams (rigid offsets, rigid links interconnecting the equivalent columns at the story levels) in correctly rendering the torsional behavior of the core: these beams must not hinder the warping of the core's cross-section. This can be achieved only in the case of classical model No. 2, while in models using only one equivalent column (No. 3 and No. 4) warping of the cross-section cannot be simulated at all (Stafford-Smith and Girgis, 1986; Avramidis, 1991).

For reasons already explained in Section 1.2, the comparison of stresses M, Q, N is performed using their resultant values for the composite cross-section. Bending moments, shear and axial forces in the equivalent columns of models No. 2 and No. 3 are transferred to the mass center of the core's cross-section according to the well-known rules for resolution, addition and transmissibility of forces.

2.4. Core modeling with panel elements (Model No. 5)

A detailed description of the panel elements used here is given in Xenidis *et al*. (1998) and Wilson and Habibullah (1992). Here, attention is drawn to the necessity of correctly modeling the torsional stiffness of the core. This can be achieved by using additional auxiliary columns at the edges of the core model. These fictitious columns should have torsional stiffnesses of appropriate magnitude, while all other sectional stiffnesses must be set equal to zero.

2.5. Core modeling with one shell element per flange and story (Model No. 6)

An alternative modeling, similar to that with panel elements, can be obtained by replacing each panel element by a finite shell element of the type described in Batoz and Tahar (1982), Taylor and Simo (1985) and Wilson and Habibullah (1992a). These shell elements combine membrane and bending behavior and incorporate all three rotational degrees of freedom at their nodes. Thus, they provide a more efficient simulation of flexural as well as of torsional deformations at element level. In order to account for the rigid diaphragm behavior of the slabs, auxiliary beams along the flanges at all story levels are used, the sectional properties of which are the same as described for Model No. 1.

3. MODEL COMPARISON AND SELECTIVE PRESENTATION OF RESULTS

3.1. Introduction

The results obtained from the analysis of the isolated core (Figure 1) and of the building structure (Figure 2) are selectively presented below. The results include static displacements and stresses, and also natural vibration periods for all models presented above (No. 1–No. 6).

The comparison and evaluation of models are based on the results from the static analysis of the isolated core (Figure 1) under strong torsional strain and also on the results from the equivalent static analysis of the 10-story building (Figure 2) for seismic loading along the *x*- and *y*-directions. Subsequently, in order to check the reliability of the various models in the case of dynamic loading, the results from a series of response spectrum analyses are used. These analyses were performed: (a) for an eccentric seismic excitation of the isolated core along the *x*-axis; and (b) for simultaneously imposed seismic excitations along the *x*- and *y*-axes of the building. In addition, the comparisons include two line-elements of the building's structural system: (a) column Σ11 on the perimeter, which is diametrically opposed to the core and is expected to perform large displacements; and (b) beam Δ1, which is coupled with the core and is expected to develop relatively large stresses.

As mentioned before, the basis for all comparisons is served by the results obtained from the analysis of the investigated structural systems using a highly accurate finite shell element model (model No. 1). Although in the present paper only results concerning the 10-story building of Figure 2 are presented, the conclusions drawn can be considered to be of wider validity because, on the one hand, they are based on a large number of investigations of various building structures as well, and because, on the other hand, they confirm similar conclusions worked out in the past concerning particular core models (Avramidis, 1991; Xenidis *et al*., 1993).

3.2. Equivalent static analysis

3.2.1. Displacements and natural periods of the isolated core.

3.2.1.1. Displacement of the stories' mass centers (Figure 4). Models No. 3 and No. 4 with one equivalent column at the shear center and at the center of mass, respectively, show very large deviations (see Figure 4). Apparently, to a large extend, these are due to the inherent inability of these models to correctly account for the warping resistance (Vlasov warping) of the composite cross-section of the core (Avramidis, 1991; Xenidis *et al*., 1998). Model No. 2 (with one equivalent column at the mass center of each flange of the core) displays a quite acceptable performance. The results for Models No. 5 (panel elements) and No. 6 (one shell element per flange and story) are practically identical with the corresponding values of Model No. 1.

3.2.1.2. Warping of the core's cross-section (Figure 5). The inability of Models No. 3 and No. 4 to simulate the warping at the top of the composite cross-section of the core is due to the fact that the

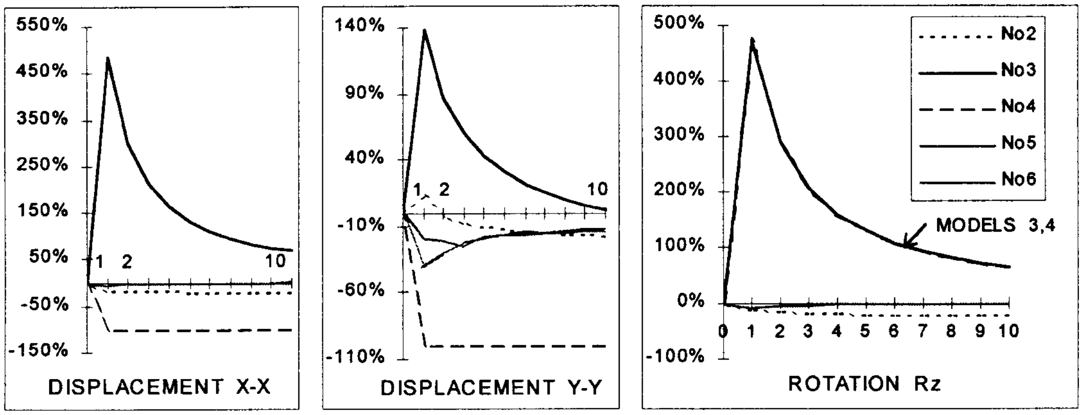

Figure 4. Percentage divergences of displacements and rotations at the stories' mass centers of Models No. 2–No. 6 with reference to Model No. 1—Equivalent static analysis

model consists of a single equivalent column. Thus, all far end nodes of the rigid links connected to the equivalent column at each story level perform dependent vertical displacements in such a way that the rigid links remain always in the same plane. From the results shown in Figure 5, Models No. 5 and No. 6 perform very well, while Model No. 2 produces values with significant deviations from the reference solution.

3.2.1.3. Natural vibration periods (Table II). The above mentioned remarks concerning the models' performance are further consolidated by results obtained for natural vibration periods. Models No. 3 and No. 4 exhibit large positive deviations for the first (fundamental) vibration period, while Models No. 2, No. 5 and No. 6 display acceptable responses.

3.2.2. Stresses of the isolated core (Figures 6 and 7). As mentioned in Section 1.2, the assessment of the modeling effectiveness was based in earlier investigations on results for the individual flanges of the core. This is not necessary any more, because of the availability of

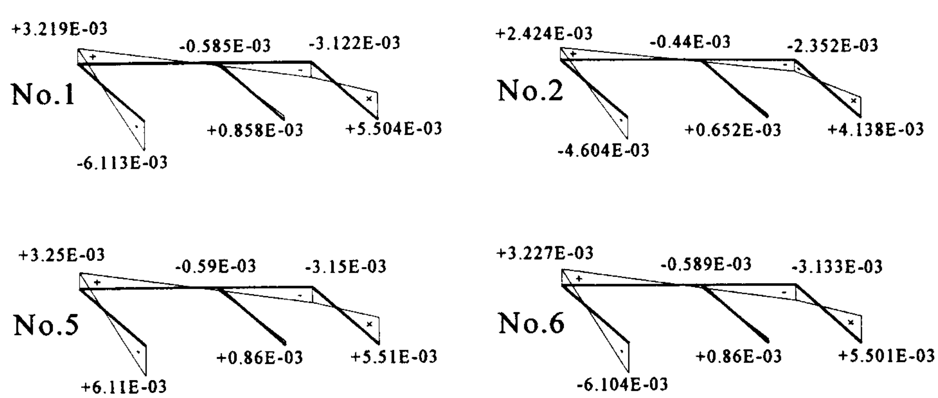

Figure 5. Warping at the open core's top for Models No. 1, No. 2, No. 5 and No. 6—equivalent static analysis (the vertical displacements are given in meters)

Table II. Natural periods of vibration of isolated cores for Models No. 1–No. 6

	No. 1	No. 2	No. 3	No. 4	No. 5	No. 6
T_1	3·823	3·315	5·534	6·433	3·652	3·646
T_2	2·042	1·986	1·847	2·147	1·956	1·953
T_3	0·925	0·864	1·111	1·979	0·868	0·866
T_4	0·525	0·513	0·932	1·291	0·498	0·499
T_5	0·379	0·379	0·803	0·934	0·347	0·348
T_6	0·340	0·332	0·638	0·742	0·313	0·313
T_7	0·205	0·218	0·538	0·626	0·185	0·188
T_8	0·144	0·147	0·506	0·552	0·117	0·121
T_9	0·124	0·127	0·474	0·504	0·113	0·114
T_{10}	0·102	0·110	0·433	0·473	0·094	0·095

professional programs allowing for dimensioning (designing and verifying) an arbitrarily shaped R/C cross-section as a whole. As already reported (Xenidis *et al*., 1998), the deviations of the overall response of the composite cross-section are definitely smaller than the deviations of the individual responses of the core's flanges. However, in the case of an isolated core, which can be regarded as a statically determinate cantilever, no such differences occur. Therefore, here, comparison of stresses for individual flanges is legitimate. In particular, the following comparisons refer to the stresses in the left flange and in the web of the isolated core (Figures 6 and 7). Models No. 3 and No. 4 proved to be of very poor effectiveness, which probably arises from their oversimplified geometry. Therefore, these two models are not further investigated. Careful comparison of the shape and ordinates of *M*-, *Q*- and N-diagrams for Models No. 2, No. 5 and No. 6 to the 'accurate' reference solution leads to the conclusion that frame Model No. 2 displays significant deviations (compare, for example, the *M*-, *Q*-, *N*- values at the higher stories of the left flange and along the full height of the core's web).

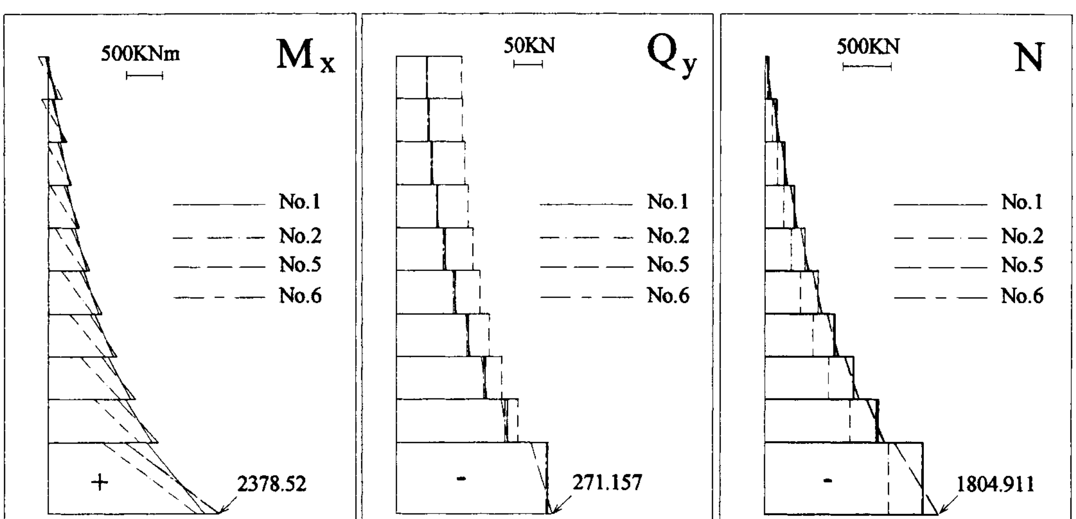

Figure 6. M-, Q-, N-diagrams for the left flange of the open core for Models No. 1, No. 2, No. 5 and No. 6—equivalent static analysis

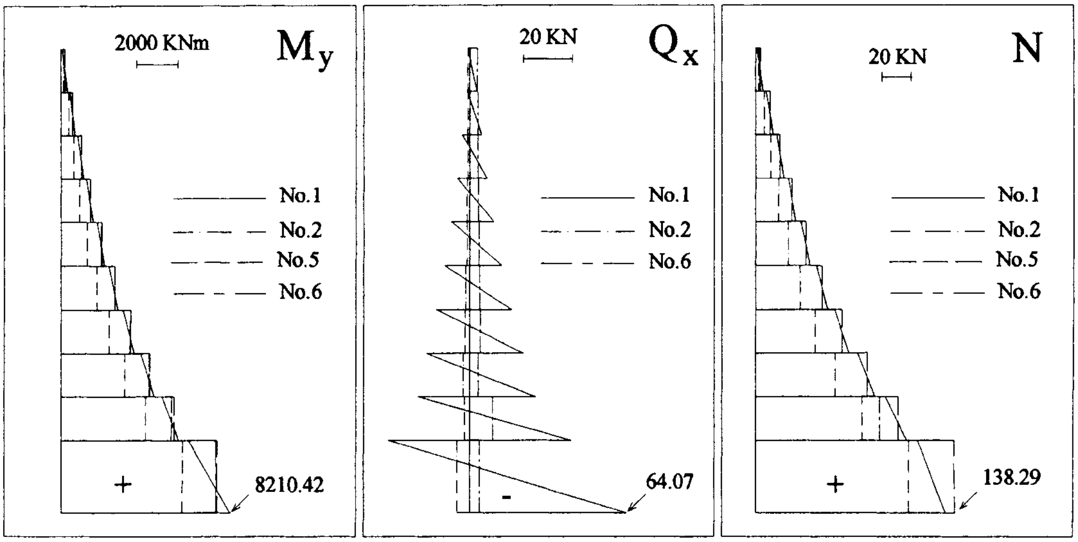

Figure 7. M-, Q-, N-diagrams for the web of the open core for Models No. 1, No. 2, No. 5 and No. 6—equivalent static analysis

3.2.3. Displacements and natural periods of the 10-story building.

3.2.3.1. Displacements of the stories' mass centers (Figure 8). Model No. 3 (one equivalent column at the shear center) is more flexible and Model No. 4 (one equivalent column at the mass center) is less flexible than the reference Model No. 1, when the seismic load acts along the x-direction (Figure 8a). For seismic excitation along the y-direction (see Figure 8b) this situation is inverted for displacements in the excitation's direction, while it is maintained for displacements orthogonal to the earthquake. It is also maintained for rotation about the vertical axis, although both models are torsionally stiffer compared with the reference model. The classical Model No. 2, although appearing a bit stiffer in both seismic directions, turns out, in general, to be more accurate than Models No. 3 and No. 4. The panel element model and the model with one shell element per flange and story (No. 5 and No. 6, respectively) also exhibit a quite acceptable behavior, with displacement values that are practically identical with the corresponding values of the reference Model No. 1.

3.2.3.2. Warping of the core's cross-section (Figure 9). The preliminary remarks and conclusions concerning the reliability of the different models as resulting from the data presented so far is further consolidated by results referring to the core's cross-section warping: Model No. 3 produces unacceptably large deviations. Model No. 2 simulates the cross-section warping quantitatively better than Model No. 4. Models No. 5 and No. 6 yield, like model No. 2, very good results.

3.2.3.3. Natural vibration periods (Table III). The results for the (coupled) natural vibration periods of the building also confirm the previous observations about the models' behavior: Models No. 2, No. 5 and No. 6 produce acceptable results of similar reliability. Among them, Model No. 2 yields the best results, giving a near zero deviation for the first (fundamental) natural period. In contrast, Models No. 3 (compare, e.g., T_2) and No. 4 (compare, e.g., T_1) show noticeable deviations.

3.2.4. Stresses of the 10-story building.

3.2.4.1. General remarks. For the reasons mentioned in Sections 1.2 and 2.3, the stresses M, Q, N are

(a)

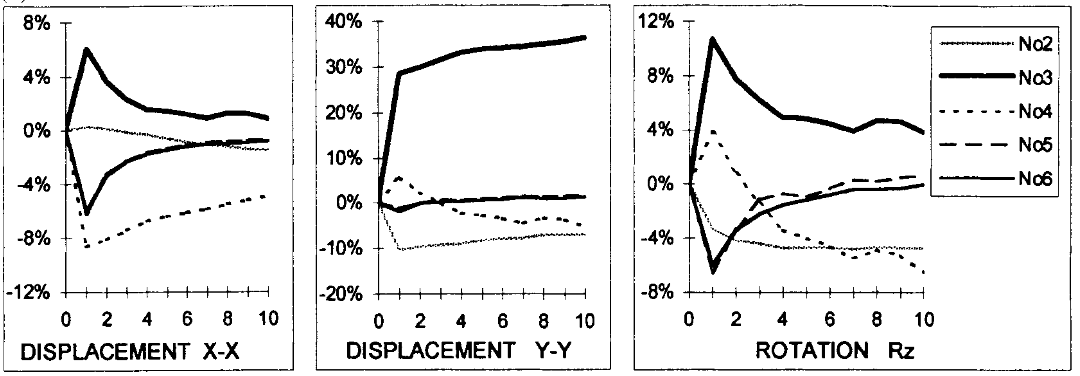

Figure 8a. Percentage divergences of displacements and rotations at the stories' mass centers of Models No. 2–No. 6 with reference to Model No. 1. Seismic loading in the *x*-direction—equivalent static analysis

(b)

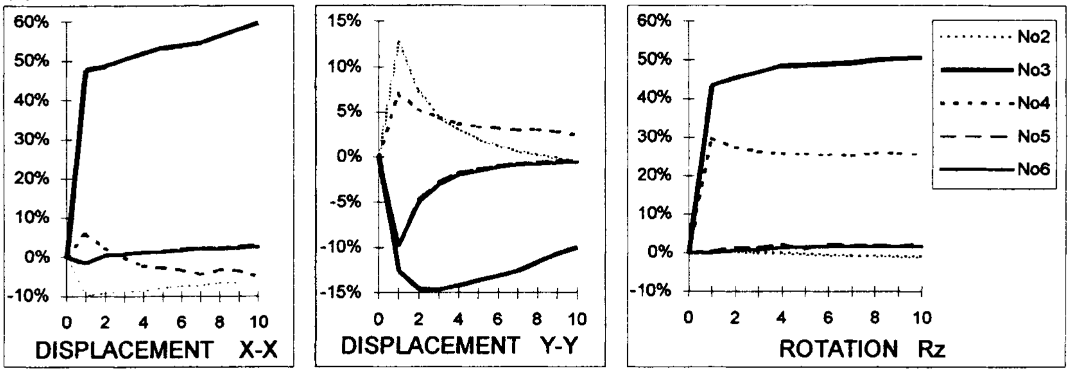

Figure 8b. Percentage divergences of displacements and rotations at the stories' mass centers of Models No. 2–No. 6 with reference to Model No. 1. Seismic loading in the *y*-direction—equivalent static analysis

given as overall (resultant) values at the mass center of the composite cross-section of the core, which is the structural subsystem causing most of the modeling problems. It is worth mentioning that calculation of reinforcements considering composite cross-section as a unit and based on the resultant cross sectional forces is much more effective than calculations of reinforcement based on sectional forces determined for each individual flange separately and carried out for its rectangular cross-section. As the latter method cannot properly account for the contribution of the co-operating widths of the actually transverse flanges, the former method must be preferred. For Models No. 4 and No. 5 the resultant values *M, Q, N* are calculated directly by the analysis programs used here, while for the other models the transfer of the *M, Q, N* to the mass center of the composite cross-section is performed according to the well-known rules of force resolution, addition and transmissibility (Xenidis *et al*., 1998).

3.2.4.2. Diagrams of sectional forces M, Q, N in column Σ*11 (Figure 10).* Figure 10 presents stresses M_y, Q_y, N in column $\Sigma 11$ for seismic excitation in the *x*-direction. Models No. 4, No. 5 and No. 6 show deviations on the unsafe side (compare, e.g., moments and shear stresses at the column's base), while Model No. 3, although displaying large fluctuations in results, generally behaves more conservatively. In contrast, Model No. 2 ('classical') produces the most satisfactory results.

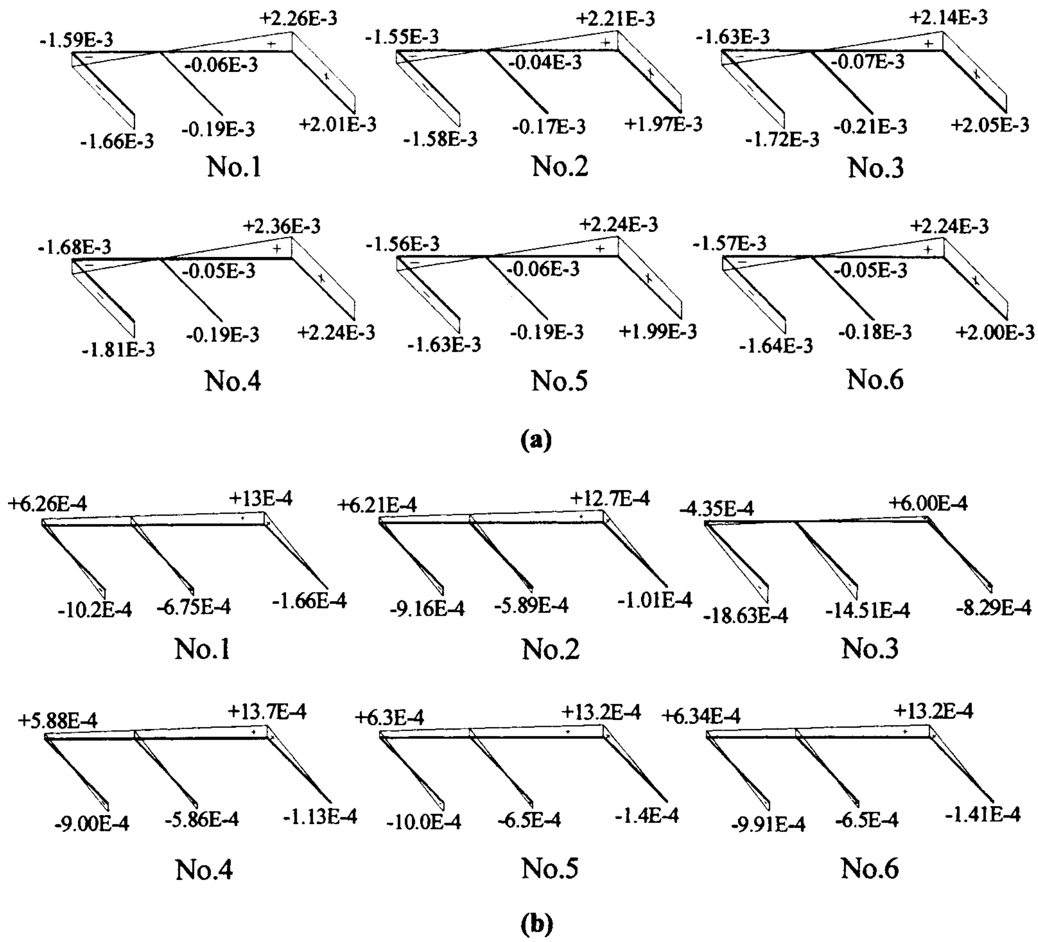

Figure 9. Warping at the core's top for Models No. 1–No. 6. Seismic loading in the *x*-direction (a) and in the *y*-direction (b)—equivalent static analysis (the vertical displacements are given in meters)

Table III. Natural periods of vibration T_i (i = 1–10) for Models No. 1–No. 6

	No. 1	No. 2	No. 3	No. 4	No. 5	No. 6
T_1	0·9812	0·9850	0·9752	1·0001	0·9758	0·9741
T_2	0·7797	0·7893	0·6898	0·7668	0·7715	0·7706
T_3	0·4708	0·4810	0·4438	0·5115	0·4663	0·4658
T_4	0·3548	0·3560	0·3579	0·3641	0·3518	0·3515
T_5	0·2449	0·2523	0·2056	0·2391	0·2392	0·2391
T_6	0·2015	0·2014	0·1865	0·2072	0·1989	0·1996
T_7	0·1344	0·1334	0·1392	0·1395	0·1310	0·1327
T_8	0·1235	0·1279	0·1093	0·1288	0·1169	0·1211
T_9	0·1207	0·1261	0·1065	0·1172	0·1145	0·1158
T_{10}	0·1033	0·1015	0·0861	0·1073	0·0986	0·1013

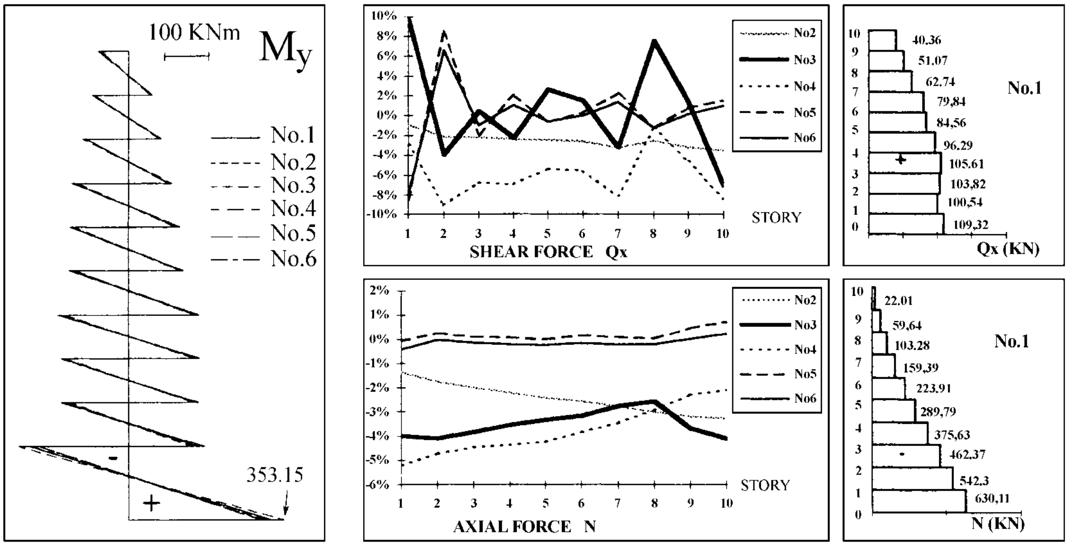

Figure 10. M_y-, Q_x-, N-diagrams for column Σ11 for Models No. 1–No. 6. Seismic loading in the x-direction—*equivalent static analysis*

3.2.4.3. Moments and shear stresses in beam Δ1 (Figure 11). Here too, Model No. 2 performs very well, as do Models No. 5 and No. 6 (compare, e.g., moments and shear stresses at the 1st story). In contrast, the equivalent frame models No. 3 and No. 4, although not exhibiting large deviations from the reference Model No. 1, are definitely less efficient compared to the other models.

3.2.4.4. Stresses in the core (Figure 12). As has been shown in previous papers (Avramiridis, 1991; Avramidis and Xenidis, 1991; Xenidis *et al*., 1992; Xenidis and Avramidis, 1992; Xenidis *et al*., 1993; Avramidis *et al*., 1997; Xenidis *et al*., 1998; Xenidis and Avramidis, 1999), results based either on oversimplified or on overcomplicated models of building cores display large deviations from the solution of the reference model as well as from each other. On the other hand, careful examination of

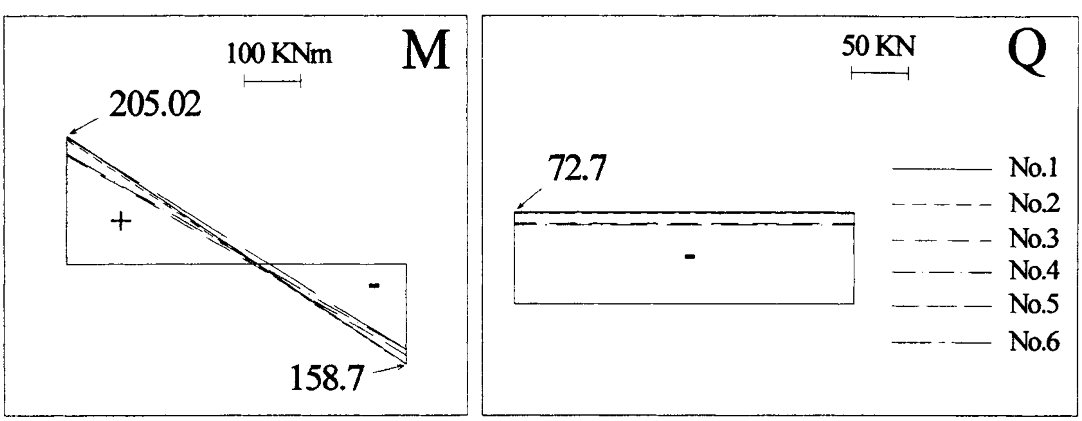

Figure 11. *M*-, *Q*-diagrams for beam Δ1 for Models No. 1–No. 6 of the 1st story of the building. Seismic loading in the x-direction—equivalent static analysis

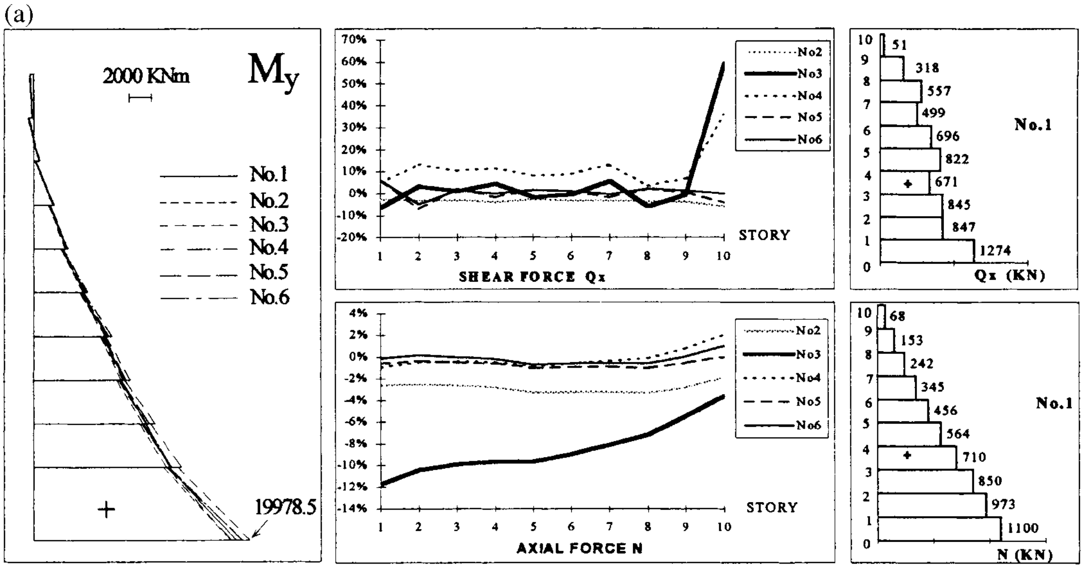

Figure 12a. M_y-, Q_x-, N-diagrams in core's cross-section for Models No. 1–No. 6. Seismic loading in the x-direction—equivalent static analysis

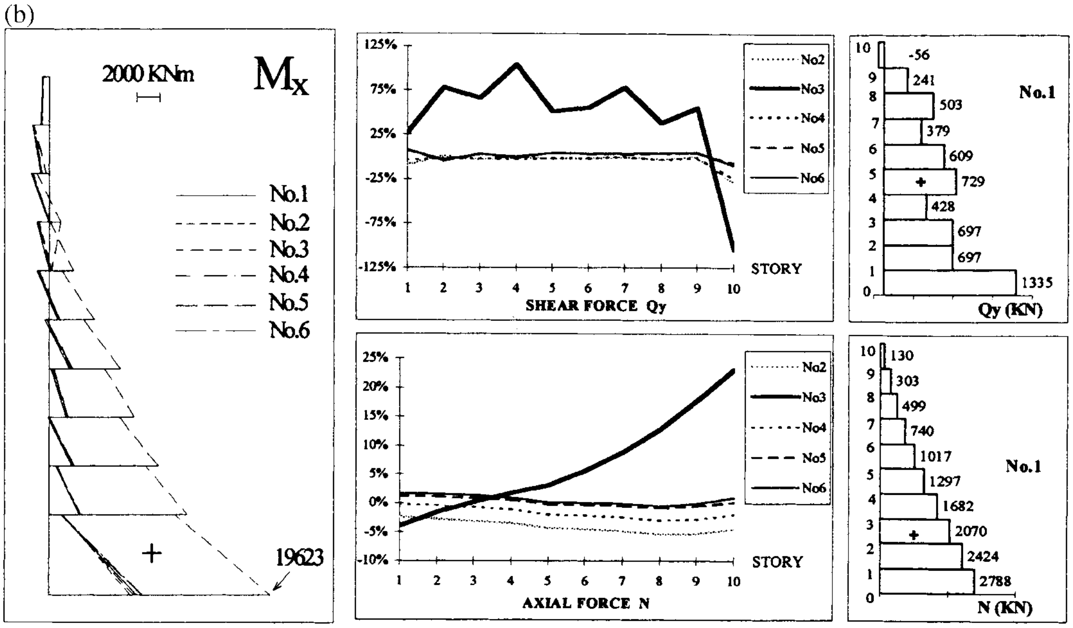

Figure 12b. M_x-, Q_y-, N-diagrams in core's section for Models No. 1–No. 6. Seismic loading in the y-direction—equivalent static analysis

shape and ordinates of the M_y-, Q_x- and N-diagrams (Figures 12 a,b) of the core investigated in this paper (as well as of a series of other cores and structural systems) leads to the general observation that discrepancies between models reduce significantly if the stress resultants of the core section as a whole are compared with each other.

Table IV. Resultant stresses in core's cross-section at 0·00 m for Models No. 1–No. 6. Seismic loading in the x-direction (a) and in the y-direction (b)—equivalent static analysis

	No. 1	No. 2	No. 3	No. 4	No. 5	No. 6
Q_x	1273·8	1240·2	1192·3	1335·2	1353·4	1351·3
Q_y	263·0	233·9	342·6	285·0	258·5	256·8
N	1100·2	1071·4	971·1	1089·5	1093·3	1098·7
M_x	1459·3	1324·9	3281·2	1301·2	1472·10	1474·9
M_y	18784·5	18188·0	18253·4	19978·5	19236·4	19249·8

	No. 1	No. 2	No. 3	No. 4	No. 5	No. 6
Q_x		−2·64%	−6·40%	4·82%	6·25%	6·08%
Q_y		−11·06%	30·26%	8·37%	−1·72%	−2·37%
N		−2·62%	−11·73%	−0·98%	−0·63%	−0·14%
M_x		−9·21%	124·85%	−10·84%	0·88%	1·07%
M_y		−3·18%	−2·83%	6·36%	2·41%	2·48%

Percentage divergences $\{(a_i - b_i)/a_i\} \times 100$ in reference to Model No. 1

(a)

	No. 1	No. 2	No. 3	No. 4	No. 5	No. 6
Q_x	336·4	340·1	529·6	416·2	360·4	360·2
Q_y	1334·8	1205·4	1702·9	1285·1	1438·6	1439·7
N	2787·7	2723·1	2679·6	2782·7	2821·5	2834·2
M_x	7714·9	7168·0	19623·0	7470·0	8180·10	8215·7
M_y	4588·4	4388·9	6360·7	4846·6	4768·5	4719·7

	No. 1	No. 2	No. 3	No. 4	No. 5	No. 6
Q_x		1·09%	57·44%	23·72%	7·13%	7·06%
Q_y		−9·69%	27·58%	−3·72%	7·78%	7·86%
N		−2·32%	−3·88%	−0·18%	1·21%	1·67%
M_x		−7·09%	154·35%	−3·17%	6·03%	6·49%
M_y		−4·35%	38·63%	5·63%	3·92%	2·86%

Percentage divergences $\{(a_i - b_i)/a_i\} \times 100$ of Models No. 2–No. 6. with reference to Model No. 1

(b)

However, in spite of this general observation, comparing *M*, *Q*, *N* at the core's basis (Table IV), where a good approximation of stresses is considered to be of great importance in engineering practice, reveals major differences between the models. More precisely, Model No. 3 (one equivalent column at the shear center) is judged to be unreliable. On the contrary, Model No. 4 and, to an even larger extend, Model No. 2 ('classical' equivalent frame), No. 5 (panel elements) and No. 6 (sparse mesh shell element model) provide acceptable results.

3.3. Response spectrum analysis

3.3.1. General remarks. It should be recalled that comparisons of displacements and stresses in the isolated core were based on results obtained for eccentric seismic excitation along the *x*-direction. On the other hand, comparisons of displacements and stresses of the 10-story building were based on results obtained for simultaneously imposed seismic excitations along the *x*- and *y*-directions using the same response spectrum, in accordance to modern seismic design codes. It should also be noted that the average deviations in the case of response spectrum analysis are generally expected to be lower than deviations in the case of equivalent static analysis. This fact is due to the better accuracy of mass modeling and mass discretization compared to the stiffness modeling and discretization of cores.

The importance of the applied modal superposition method (SRSS or CQC rule) for the achieved level of approximation for the various models should also be mentioned. When the ratio T_{i+1}/T_i of two successive natural periods approaches 1 (according to the Greek seismic design code (Manos, 1994): when $T_{i+1}/T_i > 10/(10+\xi) = 10/(10+5) = 0{\cdot}667$, where $\xi = 5$ denotes the damping ratio for R/C) application of the CQC rule is highly recommended in order to properly account for the correlation between vibration modes. Here, for the 10-story building under consideration, the first ratio T_2/T_1 as well as almost all the others are larger than 0·667 (T_3/T_2 being an exception). This can be the source of some additional deviations if the SRSS rule is used.

Finally, it must be realized that in case of response spectrum analysis it was not possible to compare core stresses directly. In order to make a comparison, the resultant cross-sectional forces in the core (or in its individual flanges) must be composed of the finite element stresses obtained from the reference Model No. 1. However, as these are spectral, i.e. maximum stresses, they do not occur simultaneously and, therefore, cannot be algebraically added to produce the resultant moments and shear and axial sectional forces. Yet, comparison of the response values of the isolated core is possible between Models No. 2 and No. 5. For comparison's sake, here the panel element Model No. 5 will be considered as the reference solution. For the 10-story building, comparisons are restricted to Models No. 4 and No. 5. For these models, the computer programs used (Wilson and Habibullah, 1992a, b) routinely calculate the resultant spectral values of moments, shear forces, and axial forces directly at the mass center of the core's cross-section.

3.3.2. Displacements of the isolated core (Figure 13). From the diagrams of spectral displacements u_x, u_y and ϕ at the mass center (Figure 13), the generally good performance of Models No. 5 and No. 6 becomes clear. Deviations of up to 30% (compare, e.g., u_x and ϕ at the top) are exhibited by the classical equivalent frame model, No. 2, while frame models No. 3 and No. 4 exhibit large deviations and must be considered as completely failing.

3.3.3. Stresses in the isolated core (Figures 14 and 15). In comparing the spectral stresses *M, Q, N* in the left flange of the core (Figure 14), equivalent frame model No. 2 exhibits large deviations

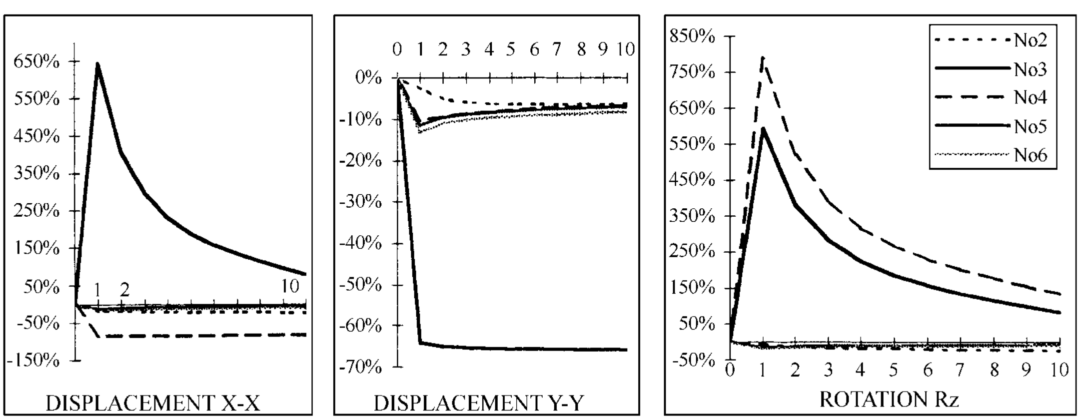

Figure 13. Percentage divergences of displacements and rotations at the stories mass center of Models No. 2 –No. 6 with reference to Model No. 1—response spectrum analysis

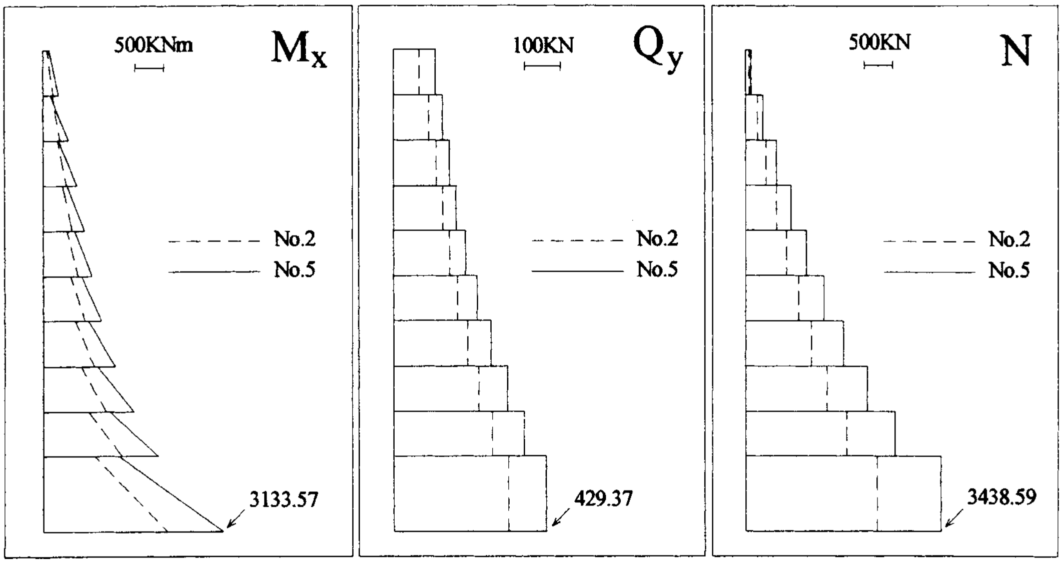

Figure 14. *M*-, *Q*-, *N*-diagrams for the left flange of the core for Models No. 2 and No. 5—response spectrum analysis

close to 50%, and, therefore, fails in comparison to panel element model No. 5. For the web of the core (Figure 15) the deviations do not exceed 20% (compare, e.g., the flexural moments at the top and at the base).

3.3.4. Displacements of the 10-story building. From the diagram in Figure 16 referring to the response spectrum analysis along the *x*- and *y*-directions, the very good agreement of displacements u_x, u_y and ϕ of the stories' mass centers of Model No. 2 ('classical') with those of the reference Model No. 1 can be seen. Equally satisfactory are the results achieved using Models No. 5 and No 6. On the contrary, frame models No 3 and No. 4, although not exhibiting large deviations, fall short (compare, e.g., displacements u_y and top story rotation of Models No. 3 and No. 4, respectively).

3.3.5. Stresses of the 10-story building. From Figure 17, showing stresses M_y, Q_x, N in column Σ11, it can be concluded that Model No. 2 behaves very satisfactorily, giving response values on the safe side compared with Model No. 1. Both panel model No. 5 and sparse-mesh shell element model No. 6 produce values on the unsafe side, while frame models No. 3 and No. 4 differ only in certain stress values (e.g., the axial force N at the column's base for Model No. 5, the flexural moment M_y at the column's base for Model No. 4).

Similar observations can be made when comparing the diagrams for beam Δ1 (Figure 18). Models No. 2, No. 5, and No. 6 produce responses very close to that of the reference model, No. 1, while both frame models No. 3 and No. 4 display inaccuracies (compare, e.g., moments and shear stresses at the top floor).

Finally, concerning the core's stresses, the comparison is restricted to Models No. 5 (panel element) and No. 4 (with one equivalent column at the mass center) for the reasons mentioned in Section 3.3.1 (Figure 19). The deviations of the latter model with respect to the former lie between 11 and 22% (compare, e.g., M_x at the core's base and Q_x at the top floor).

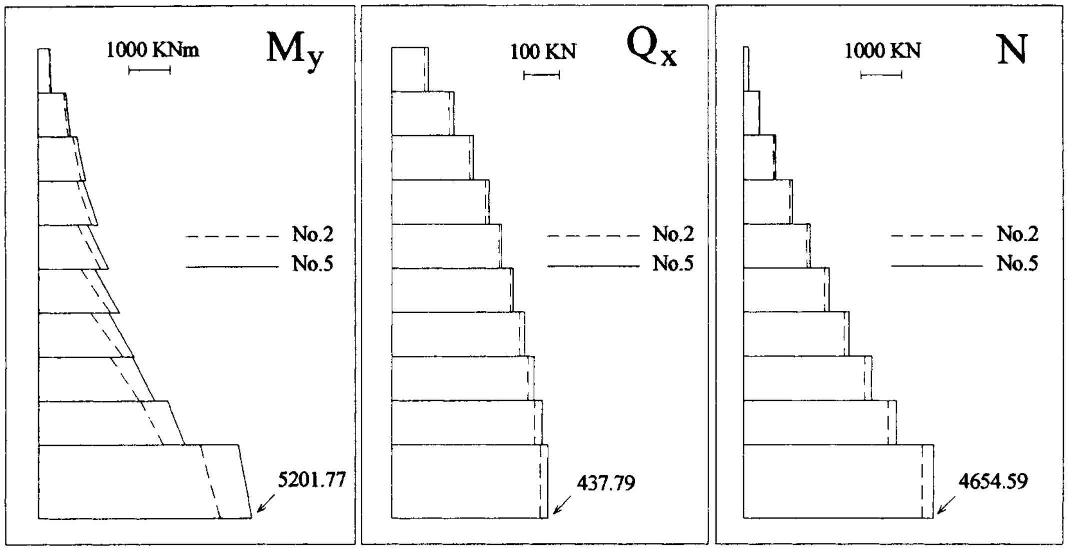

Figure 15. *M*-, *Q*-, *N*-diagrams for the web of the core for Models No. 2 and No. 5—response spectrum analysis

4. CONCLUSIONS

As mentioned in the Introduction, the present investigation concerns, in the first place, isolated cores and aims at determining the maximum deviations produced by the various simplified structural models. In practice, the core is usually surrounded by and connected to a frame, representing the rest of the building structure. This surrounding frame can be generally modelled with greater accuracy than the core itself. Therefore, the deviations of the whole building model tend to be generally smaller than the deviations observed when analysing isolated cores. Results and conclusions in this paper refer to open two-cell cores and cannot be extended to cores of different geometry and shape without additional investigations.

Summarizing all observations and comparative remarks made above, the following conclusions can

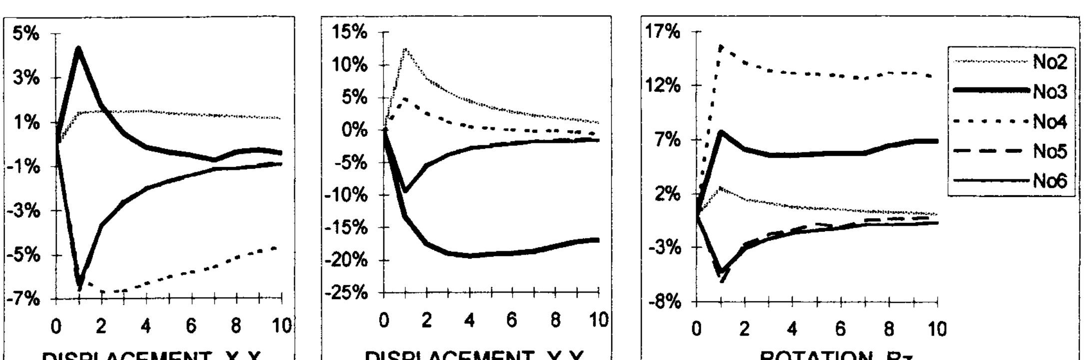

Figure 16. Percentage divergences of displacements and rotations at stories' mass center of Models No. 2–No. 6 with reference to Model No. 1—response spectrum analysis

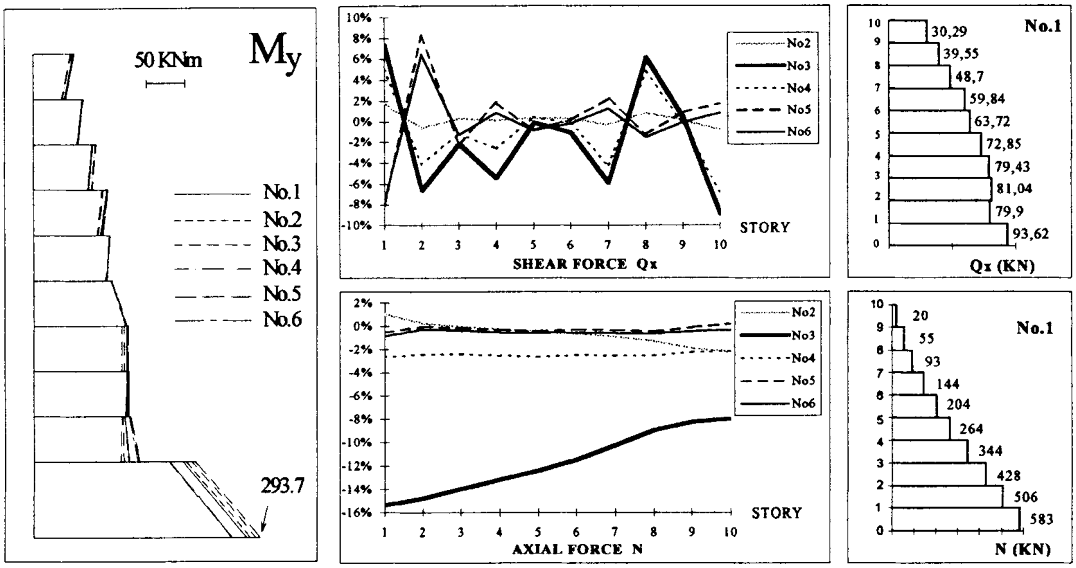

Figure 17. M_y-, Q_x-, N-diagrams for column Σ11 for Models No. 1–No. 6—response spectrum analysis

be formulated concerning both methods of analysis, the equivalent static and the response spectrum methods.

(a) *Isolated core.* The highly simplified Models No. 3 and No. 4 are not capable of simulating the structural behavior of the core. Because of the major deviations in displacements and natural vibration periods, these models are considered to be of very limited reliability. On the other hand, Model No. 2 behaves rather well with acceptable values for deformations and natural vibration periods. Yet, when comparing stresses, some significant deviations are observed. Finally, Models No. 5 and No. 6 do not show serious deviations from the reference solution, neither in terms of deformations and natural vibration periods nor in terms of stresses.

(b) *10-story building*. The classical equivalent frame model, Model No. 2 produces, in general, the smallest deviations and proves to be very close to the reference model, Model No. 1. Very good

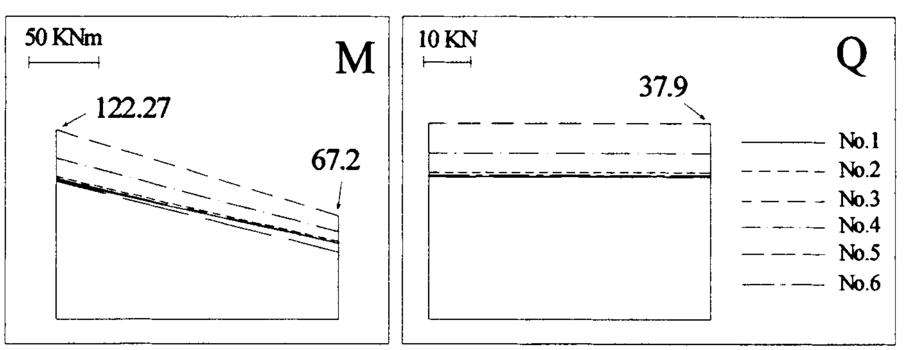

Figure 18. M-, Q-diagrams for beam Δ1 of the 10th story of the building for Models No. 1–No. 6—response spectrum analysis

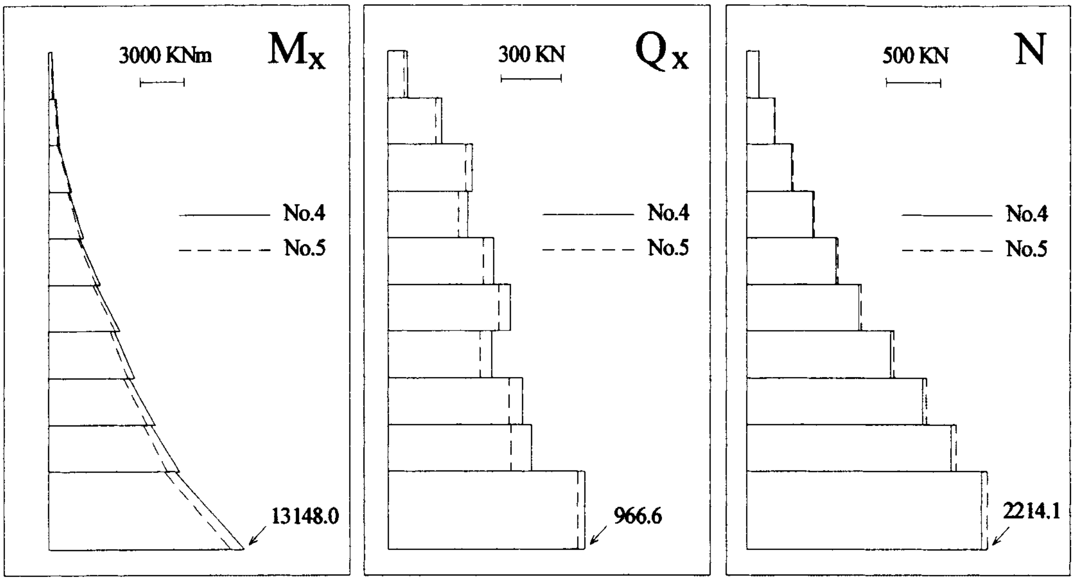

Figure 19. M_x-, Q_x-, N-diagrams at the mass center of the core's composite section for Models No. 4 and No. 5—response spectrum analysis

results are produced by Models No. 5 (panel elements) and No. 6 (one shell element per flange and story) for all response quantities (displacements, natural vibration periods and resultant stresses in the core's composite cross-section). Less effective, but nevertheless marginally acceptable, is Model No. 4 with one equivalent column at the mass center of the core. On the contrary, Model No. 3 with one equivalent column at the core's shear center gives very poor results and must not be used in modeling cores.

REFERENCES

Avramidis IE. 1991. Zur Kritik des äquivalenten Rahmenmodells für Wandscheiben und Hochhauskerne. *Bautechnik* **68**(H.8): S.275–285.

Avramidis IE, Triamataki M, Xenidis H. 1997. Simplified models for R/C building cores. Development, systematic comparison and performance evaluation for static and dynamic loading. Research Report, Institute of Applied Statics, Department of Civil Engineering, Aristotle University of Thessaloniki, Greece.

Avramidis IE, Xenidis H. 1991. Systematic investigation of the deficiencies of equivalent frame models for open R/C cores. *Proceedings of the 10th Greek Concrete Conference*, Corfu; 179–186.

Batoz JL, Tahar MB. 1982. Evaluation of a new quadrilateral thin plate bending element. *International Journal for Numerical Methods in Engineering* **18**: 1655–1667.

Beck H. 1962. Contribution to the analysis of coupled shear walls. *ACI Journal, Proceedings* **V.59**(8): 1055–1070.

Girgis AM, Stafford-Smith B. 1979. Torsion analysis of building cores partially closed by beams. *Proceedings of the symposium on the Behaviour of Building Systems and Components*, Vanderbilt University, Nashville; 211–227.

Heidebrecht AC, Swift RD. 1971. Analysis of asymmetrical coupled shear walls. *ASCE, Journal of the Structural Division* **97**(ST5): 1407.

Lew IP, Narov F. 1983. Three dimensional equivalent frame analysis of shear walls. *Concrete International: Design & Construction* **5**(10): 25–30.

MacLeod IA. 1967. Lateral stiffness of shear walls with openings in tall buildings. In *Tall Buildings*. Pergamon: London: 223–244.

MacLeod IA. 1973. Analysis of shear wall buildings by the frame method. *Proceedings of the Institution of Civil Engineers* **55**: 593–603.

MacLeod IA. 1976. General frame element for shear wall analysis. *Proceedings of the Institution of Civil Engineers* **61**(Part 2): 785–790.

MacLeod IA. 1977. Structural analysis of wall systems. *The Structural Engineer (London)* **V.55**(11): 487–495.

MacLeod IA, Green DR. 1973. Frame idealization for shear wall systems. *The Structural Engineer (London)* **V.51**(2): 71–74.

MacLeod IA, Hosny HM. 1977. Frame analysis of shear wall cores. *ASCE, Journal of the Structural Division* **103**(ST10): 2037–2047.

Manos G. 1994. Provisions of the new Greek seismic code. In *International Handbook of Earthquake Engineering*, Paz M. (ed.). Chapman & Hall: London: 239–248.

Schwaighofer J. 1969. Ein Beitrag zum Windscheiben-Problem. *Der Bauingenieur* **44**(10): 370–373.

Schwaighofer J, Microys HF. 1969. Analysis of shear walls using standard computer programs. *ACI Journal, Proceedings* **66**(12): 1005–1007.

Stafford-Smith B, Abate A. 1981. Analysis of non-planar shear wall assemblies by analogous frame. *Proceedings of the Institution of Civil Engineers* **71**(Part 2): 395–406.

Stafford-Smith B, Girgis AM. 1984. Simple analogous frames for shear wall analysis. *ASCE, Journal of the Structural Division* **110**(11): 2655–2666.

Stafford-Smith B, Girgis AM. 1986. Deficiencies in the wide column analogy for shear wall core analysis. *Concrete International*: 58–61.

Taylor RL, Simo JC. 1985. Bending and membrane elements for analysis of thick and thin shells. *Proceeding of the NUMETA 1985 Conference* Swansea, 7–11 January.

Wilson EL, Habibullah A. 1992a. SAP90, a series of computer programs for the finite element analysis of structures. *User Manual*, Revised May 1992, Computers and Structures Inc. Berkeley, California, USA.

Wilson EL, Habibullah A. 1992b. ETABS, the three dimensional analysis of building systems, Version 5·4., Revised August 1992, California, Berkeley, USA.

Xenidis H, Athanatopoulou A, Avramidis IE. 1992. Equivalent frame modeling of shear wall cores under earthquake loading. *ICES '92, International Conference on Computational Engineering Science*, Hong-Kong, 17–22 December.

Xenidis H, Athanatopoulou A, Avramidis IE. 1993. Modeling of shear wall cores under earthquake loading using equivalent frames. *EURODYN' 93, 2nd European Conference on Structural Dynamics*, Trondheim, Norway; 901–910.

Xenidis H, Athanatopoulou A, Avramidis IE. 1994. Equivalent frame modeling of staged R/C shear walls under static and seismic loading. *Proceedings of the 11th Greek Concrete Conference*, Corfu; 399–410.

Xenidis H, Avramidis IE. 1992. Documentation of intrinsic deficiences of equivalent frame modeling of semi-opened and closed R/C cores. *Proceedings of the 1st Greek Conference on Earthquake Engineering and Engineering Seismology*, Athens: 96–105.

Xenidis H, Avramidis IE. 1999. Comparative performance of code prescribed analysis methods for R/C buildings with shear wall cores. *Proceedings of EURODYN' 99, 4th Eurpoean Conference on Structural Dynamics*, Prague, Czech Republic: 869–875.

Xenidis H, Avramidis IE, Triamataki M. 1998. Comparative performance of simplified models for R/C building cores under static and dynamic loading. *Technical Chronicle No. 3*, Technical Chamber of Greece, Athens.